ACS OMEGA

Open Access

http://pubs.acs.org/journal/acsodf

Article

Charge-Assisted Anion−π Interaction and Hydrogen Bonding Involving Alkylpyridinium Cations

Emmanuel Bitega, Reva Patil, Matthias Zeller, and Sergiy V. Rosokha*

Cite This: *ACS Omega* 2024, 9, 43058−43067

Read Online

ACCESS | Metrics & More | Article Recommendations | Supporting Information

ABSTRACT: Competition and cooperation of charge-assisted anion−π interactions and hydrogen bonding were explored in the solid state and in solutions of 1-ethyl-4-carbomethoxypyridinium iodide, the compound utilized by Kosower to calculate solvent polarity Z-indices. X-ray structural analysis of this salt revealed multiple short contacts of iodide anions with hydrogen atoms and aromatic rings of pyridinium cations. Geometric characteristics, quantum theory of atoms in molecules (QTAIM), and noncovalent interaction (NCI) analysis of these contacts indicated comparable interaction energies of the anion−π and hydrogen bonding between iodide and pyridinium cation. ^{1}H NMR (indicating the presence of the hydrogen-bonded complexes) and UV−vis measurements (which were consistent with the formation of anion−π associations) pointed out that both these supramolecular interactions also coexist in solutions. The comparable interaction energies (ΔE) of these modes were confirmed by the DFT computations. Also, while the variations of ΔE with the dielectric constant of the solvents for the complexes of iodide with the neutral π-acceptors were related to the increase of the effective radii of hydrogen- or anion−π bonded iodides, the changes in ΔE for the complexes with pyridinium followed interaction energies between two unit charges. However, the distinction of the bonding in hydrogen-bonded and anion−π complexes of iodide with pyridinium led to a switch of their relative energies with an increase of the polarity of the medium.

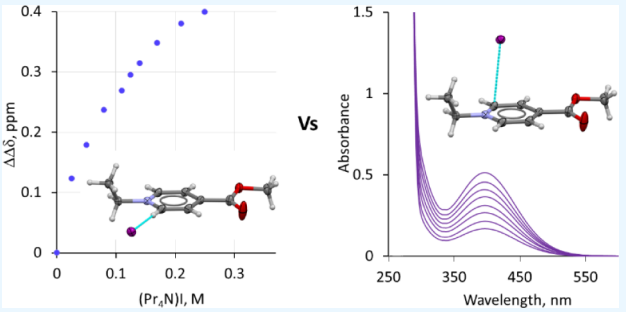

1. INTRODUCTION

Anion−π interactions became one of the focal points of supramolecular chemistry after seminal computational works were published in the early 2000s.[1−8] Yet, the examples of the systems showing this counterintuitive attraction of anions to the π-systems could be found in the articles describing charge-transfer complexes published more than 50 years ago.[9−11] Indeed, after the identification of complexes between diiodine and aromatic molecules in solutions in 1949 by Benesi and Hildebrandt and the structural characterization of molecular associations in the solid state in the 1950s by Hassel and coworkers, the study of the charge-transfer complexes attracted the attention of many researchers.[12−15] In particular, the association between various π-acceptors, e.g., trinitobenzene, tetracyanoethylene and *p*-chloranil, and halides and thiocyanate anions (which are good electron donors) were described by Briegleb et al. in 1962.[9,10] Follow-up work by Davis demonstrated that the energies of the absorption bands of such complexes are directly related to solvent polarity indices, such as Kosower's "Z" numbers.[11,16] The latter was established a few years earlier based on the solvent dependence of the energy of the UV−vis absorption band of 1-ethyl-4-carbomethoxypyridinium iodide.[16] Kosower identified this absorption band as a charge-transfer transition in the complex between iodide and the pyridinium cation, KS$^+$ (shown in Scheme 1). Most notably, he suggested that iodide anions are arranged over the face of the aromatic ring of the cationic π-acceptors in their complex. As such, using current terminology, these dyads could be considered charge-assisted anion−π complexes.

Scheme 1. Structures and Acronyms of the π-Acceptors

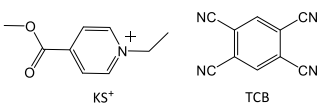

It should be mentioned, however, that the interaction of anions with the face of the π-system is not the only possible arrangement in these complexes. The anions can also approach the pyridinium π-acceptors from the side of the aromatic ring and interact with its substituents. In particular, the presence of the hydrogen substituents on the aromatic ring and in the ethyl and carbomethoxy substituents in KS$^+$ suggests the possibility of hydrogen bonding (HyB) between iodide and the pyridinium cation. Indeed, as expected for a cationic species,

Received: July 22, 2024
Revised: August 16, 2024
Accepted: September 30, 2024
Published: October 8, 2024

electrostatic potentials (calculated at the 0.001 au electron density) are positive over the surface of KS^+. The area of the maximum value of this potential (shown in Figure 1 in the potential range from 0 to 0.2 au) is located between the methylene and aromatic hydrogens (in ortho-position relative to the nitrogen atom). There is also a π-hole on the face of the aromatic ring with a potential about 10% lower than that observed on its side. This suggests that there can be at least two local minima in the potential energy landscape of the complexes between KS^+ and anions. It is surprising, however, that despite the applications of "Z" numbers as empirical measures of the solvent polarity (and the commercial availability of 1-ethyl-4-carbomethoxypyridinium iodide), definitive structural features of these complexes and conclusive evidence about the nature of the interaction between anions and pyridinium cations in these associations are lacking. Furthermore, while the literature contains many structures of salts of alkylpyridinium cations and iodide anions, the corresponding publication were focused on hydrogen or halogen bonding, if any, in these systems.[17]

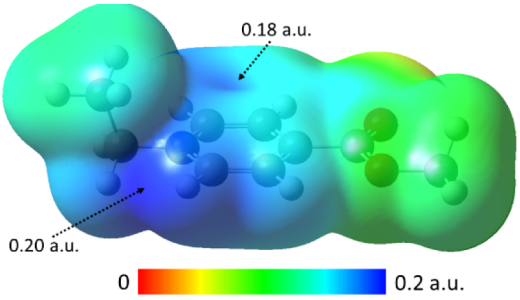

Figure 1. Surface electrostatic potential of KS^+ (at 0.001 au electron density).

In the current work, we turn to X-ray structural characterization, spectral studies, and computational analysis of the complexes of 1-ethyl-4-carbomethoxypyridinium with iodide and several other anions. Besides historical interest in the clarification of the nature of the interaction underlying Kosower's Z-indices of solvent polarity, a characterization of these associations allows us to explore the completion and/or cooperation of the two important modes of supramolecular interactions, anion$-\pi$ and hydrogen bonding between anions and cationic aromatic molecules. To reveal the distinctions between such charge-assisted bonding from that formed by anions with neutral π-acceptors, we compared the bonding of iodide with KS^+ with that of the tetracyanobenzene (TCB, Scheme 1). This neutral π-acceptor was chosen since, similarly to KS^+, it can form HyB and anion$-\pi$ complexes with anions, and both these types of associations of TCB were reported earlier.[18,19] Furthermore, the reduction potential of KS^+ (E_{red}^{o} = −0.75 V vs SCE)[20] is close to that of TCB (E_{red}^{o} = −0.65 V vs SCE.[19] Since the reduction potential (which reflects electron acceptor properties of the π-systems) represents one of the main factors determining the strength of anion$-\pi$ bonding,[19,21] the similarity of these characteristics allows us to focus on the distinctions related to the charge of the π-acceptor. Thus, a comparison of the characteristics of the anion$-\pi$ complexes with KS^+ and TCB makes it possible to establish the role of charge on the strength and characteristics of the competing hydrogen bonding and anion$-\pi$ interactions.

2. METHODS

Commercially available 1-ethyl-4-carbomethoxypyridinium iodide, (KS)I and sodium tetrakis(3,5-trifluoromethylphenyl)-borate NaBArF, were used without additional purification. Tetraalkylammonium salts of halides, thiocyanate, hexafluorophosphate, tetrafluoroborate, triflate, and perchlorate were purified by recrystallization. Dichloromethane and acetonitrile were distilled over P_2O_5 under an argon atmosphere. (KS)BArF was synthesized by adding a solution of 0.298 g (1.00 mmol) of (KS)I in dichloromethane to a solution of 0.888 g (1.00 mmol) of NaBArF in dichloromethane. The mixture was stirred for 30 min, and the NaI precipitate was filtered off. The filtrate was washed twice with water, dried, and dichloromethane was evaporated under reduced pressure, and the residue was dissolved in 30 mL of methanol. The addition of water (in a 1:1 ratio) resulted in the formation of a white precipitate of (KS)BArF, which was filtered, washed with water and dried under air. Yield 0.58 g (65%). Analysis (%): calk. for $C_{41}H_{24}BF_{24}NO_2$: C, 47.84; H, 2.35; N 1.36. Found: C, 47.89; H, 2.30; N 1.31. Mp 107−109 °C. ^{1}H NMR (400 MHz, CD_3CN) δ (ppm): 8.82 (d, 2H), 8.39 (d, 2H), 7.66 (s, 4H), 7.64 (s, 8H), 6.60 (q, 2H), 3.98 (s, 3H), 1.58 (t, 3H). The FT-IR spectrum of (KS)BArF is shown in Figure S1.

Single crystals of (KS)I and (KS)BArF were prepared by cooling solutions containing these salts in acetonitrile and methanol, respectively, and slow evaporation of these solutions at −30 °C (analogous crystals of (KS)I were also obtained from dichloromethane). The X-ray measurements were carried out on a Bruker AXS D8 Quest diffractometer with a molybdenum radiation X-ray tube (λ = 0.71073 Å). Reflections were indexed and processed, and the files were scaled and corrected for absorption using APEX4.[22] The space groups were assigned using XPREP within the SHELXTL suite of programs, the structures were solved by dual methods using ShelXT and refined by full-matrix least-squares against F^2 with all reflections using Shelxl2019 with the graphical interface Shelxle.[23,24] X-ray structures of (KS)I and (KS)BArF are shown in Figure S2. Crystallographic, data collection, and structure refinement details are listed in Table S1. Complete crystallographic data, in CIF format, have been deposited with the Cambridge Crystallographic Data Centre. CCDC 2344693 and 2344694 contain the supplementary crystallographic data for this paper. These data can be obtained free of charge via www.ccdc.cam.ac.uk/data_request/cif.

The formation of complexes between KS^+ and various anions was studied via UV−vis and ^{1}H NMR measurements in acetonitrile as described earlier (see the Supporting Information for details)[25,26] using a series of solutions with variable concentrations (from 0 to 0.4 M) of anions and constant (2−10 mM) concentrations of (KS)BArF (the spectrum of (KS)BArF does not contain any absorption bands with λ_{max} > 300 nm, and the bulky noncoordination nature of the $BArF^-$ minimizes its interference of the study of the interaction of KS^+ with the anions.[27,28] The ^{1}H NMR spectrum of (KS)BArF was essentially invariant (within 0.01 ppm) when its concentration varied from 0.5 mM to 50 mM, which confirmed the absence of the (hydrogen-bonded) self-association of KS^+.

Geometries of the complexes were optimized without constraints via M06-2X/def2-tzvpp calculations using the Gaussian 09 suite of programs.[29−31] The absence of imaginary frequencies confirmed that the optimized structures represent true minima. Calculations with various solvents as the media

https://doi.org/10.1021/acsomega.4c06750
ACS Omega 2024, 9, 43058−43067

were done using a polarizable continuum model.[32] An earlier analysis demonstrated that intermolecular associations are well-modeled using this method.[25,26,33,34] The def2-tzvpp basis set does not include a diffuse function since previous analysis demonstrated that very similar results were obtained in the modeling of noncovalent interactions involving anions with the triple-ζ basis sets with and without diffuse functions.[35] Binding energies, ΔE were determined as $\Delta E = E_C - (E_A + E_X)$, where E_C, E_A, and E_X are sums of the electronic energy and zero-point energy (ZPE) of the optimized complex, pyridinium cation and anion. Energies of the optimized complexes and their components are listed in Table S2. (Due to the absence of the minimum-energy structures showing hydrogen bonding in the gas phase and argon, energy of such complexes were estimated using the structures obtained via optimizations with the fixed C−H···I angle.) The UV−vis spectra were obtained via TD-DFT calculations of the complexes and their components optimized in the corresponding solvent. The ^{1}H NMR spectra of these species were obtained using the NMR = GIAO keyword. To check the effects of hydrogen bonding of iodide with solvent molecules on the energetics and spectra of the anion−π and HyB complexes of iodide with KS$^+$, the results of the calculations of the KS$^+$ I$^-$ pairs were compared to those of the associations between iodide, pyridinium cations and three methanol molecules hydrogen-bonded to the anion. Quantum theory of atoms in molecules (QTAIM)[36,37] and noncovalent indices (NCI)[38] analyses of the solid-state associations were performed (using atomic coordinates extracted from the X-ray structures) with Multiwfn and visualized using VMD programs.[39,40] The NCI setting was: isovalue = 0.5, color-coded with sgn(λ_2)ρ in the range from −0.04 au (blue, strong attractive interaction) to 0.02 au (red, strong nonbonded overlap).

3. RESULTS AND DISCUSSION

3.1. X-ray Structural and Computational Analysis of the Solid-State Interaction of Iodide and KS$^+$. Slow evaporation of a solution of 1-ethyl-4-carbomethoxypyridinium iodide, (KS)I, in acetonitrile or dichloromethane (see Methods) produced crystalline orange plates suitable for the single-crystal X-ray analysis. A fragment of the X-ray structure of this salt is shown in Figure 2.

The structure in Figure 2 shows multiple contacts between iodide anions and pyridinium cations which are shorter than the van der Waals separations. Most of these contacts involve hydrogen substituents of KS$^+$ which are close to the (formally positive) nitrogen atoms (Table 1).

In particular, iodides form short contacts with hydrogens at the ortho-position to the nitrogen atom of the pyridinium ring and the methylene group of the N-ethyl substituents. The geometric characteristics of these contacts (distances that are smaller than the sum of the van der Waals radii[41] and the C−H···I angles are given in Table 1) are consistent with moderately strong hydrogen bonding between pyridinium cations and iodide anions. Most important for the current work, however, was the fact that the (KS)I salt comprised contacts between I$^-$ anions and the carbon atoms in the aromatic ring of the pyridinium cations, suggesting an attraction of iodides to the π-system. It should be mentioned in this respect that there are different views of the meaning of the term "anion−π bonding" in the literature, and, in contrast to many other novel types of supramolecular bonding (e.g., halogen or chalcogen bondings), there is no IUPAC definition

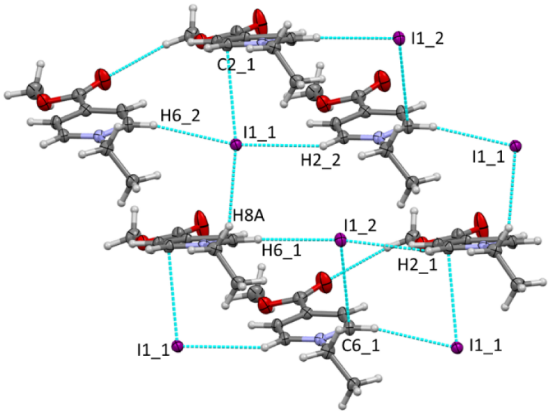

Figure 2. A fragment of the X-ray structure of (KS)I salt showing short contacts (light blue lines) between iodide anions and hydrogen substituents or aromatic ring of pyridinium cations. Appended numbers indicate atoms belonging to the first or second crystallographically independent ion pairs of the crystal structure.

of anion−π interaction.[8] Some researchers consider that anion−π interaction require positioning of the anions over the center of the aromatic rings (i.e., η_6 bonding of anion with the atoms in the aromatic ring).[43] However, the analysis of a variety of complexes of anions with distinct π-acceptors led to a broader approach to anion−π bonding, which includes η_1 to η_6 bonding of anions with one to six atoms of the ring.[1,8] Thus, while within the framework of the narrow definition, the η_1 bonding in the (KS)I salt could be defined as anion−π(C) interaction, we follow herein the more general view, and refer to the interaction of iodide with carbon as anion−π bonding.

To confirm the presence of anion−π bonding (since the I···C contacts can also be serendipitous results from crystal packing) and to compare its strength with that of the hydrogen bonding, we carried out analyses of these solid-state associations using quantum theory of atoms in molecules (QTAIM) and noncovalent interaction (NCI) indices.[36,37] Bader's QTAIM provides a powerful methodology to classify and quantify intermolecular interactions through the analysis of the topology of the electron and energy densities $\rho(\mathbf{r})$ at (3, −1) bond critical points (BCPs).[37] The presence and characteristics of BCPs in the supramolecular associations, including the magnitude of electron density $\rho(\mathbf{r})$, the Laplacian of electron density, $\nabla^2\rho(\mathbf{r})$, kinetic energy and potential energy densities $G(\mathbf{r})$ and $V(\mathbf{r})$, and energy density $H(\mathbf{r}) = G(\mathbf{r}) + V(\mathbf{r})$ allow assignments of the bonding ranging from shared-shell (SS) covalent to weak closed-shell (CS) noncovalent interactions[44−46] The QTAIM analyses of the cluster extracted from the X-ray structure of (KS)I revealed BCPs along the bond paths corresponding to each of the short contacts between iodides and hydrogen substituents or aromatic rings of pyridinium cations (Figure 3).

The QTAIM analysis shows bond paths from each nonequivalent iodide to two aromatic rings. One of these paths corresponds to the close contact between iodide and rings shown in Figure 2, and another path (and BCP) connects the iodide with the rings on the opposite side of the anion. The distances I1_2···C2_2 of 3.702 Å and I1_1···N_1 of 3.853 Å are close to the van der Waals separations of these atoms (they are shorter than the latter if the van der Waals radii of iodine of 2.17 Å proposed recently is used instead of Bondi's value of 1.98 Å.[41,47]

https://doi.org/10.1021/acsomega.4c06750
ACS Omega 2024, 9, 43058−43067

Table 1. Characteristics of the Short Contacts in the Solid-State (KS)I Salt

Contact[a]	d(I···X), Å	∠I···X−C, deg	$10^3\rho(\mathbf{r})$, au	$10^4H(\mathbf{r})$, au	$-E$, kcal/mol[b]
I1_1 ··· C2_1	3.636	4.0[c]	8.0	6.1	1.2
I1_1 ··· H6_2	3.020	160.1	8.7	8.8	1.3
I1_1 ··· H2_2	3.109	133.8	7.8	7.9	1.2
I1_1 ··· H8_A	3.054	137.2	9.0	7.5	1.4
I 1_2··· C6_1	3.558	6.1[c]	8.8	6.0	1.3
I 1_2··· H2_1	3.001	174.2	8.9	8.8	1.3
I 1_2··· H6_1	3.162	129.6	7.3	7.3	1.1

[a]See Figure 2. [b]Calculated based on the energy density, $E = 1/2V(r)$.[42] [c]Angle between the I−C bond and perpendicular to the pyridinium plane.

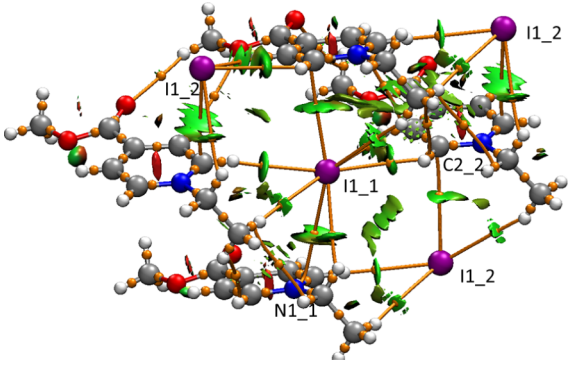

Figure 3. QTAIM and NCI analyses of the structure of (KS)I. Orange lines and small orange spheres show bond paths and BCPs and blue-green areas indicate bonding interactions.

The attractive interaction revealed by QTAIM was confirmed by the NCI analyses (which determines whether an interaction is attractive or repulsive based on the deviations of the reduced gradient of density in the system from that for a homogeneous electron gas).[38] It shows blue-green areas (corresponding to the negative values of sign(λ_2) and indicating attractive interactions) located around BCPs (Figure 3). Thus, the combination of QTAIM and NCI verified the attraction of iodide anions to the aromatic rings and hydrogen substituents located near the nitrogen atom in the pyridinium cations. Electron and energy densities, $\rho(\mathbf{r})$ and $H(\mathbf{r})$, at BCPs along the bond paths corresponding to the short contact in Figure 2 obtained from the QTAIM analyses of the (KS)I structure are listed in Table 1 (the values of $\nabla^2\rho(\mathbf{r})$, $G(\mathbf{r})$, and $V(\mathbf{r})$ are listed in Table S3). The values of electron density at all these BCPs are close to 0.01 au which is common for noncovalent bondings. Since electron densities are correlated with the strength of bonding,[37,42,48,49] the values of $\rho(\mathbf{r}) = (8 \pm 1) \times 10^{-3}$ au for all contacts suggests comparable interaction energies for HyB and anion−π bonding in the (KS)I salt. The very small positive values of energy density $H(\mathbf{r})$, which vary between 6×10^{-4} au and 9×10^{-4} au, also indicate a weak interaction related primarily to mostly electrostatic attraction.

Earlier publications also showed a close correlation of the interaction energies E and potential and/or kinetic energy densities at BCPs.[37] They led to proposal of several formulas relating energies to these characteristics (and the analysis showed that different types of interactions might require different coefficients).[42,48−51] The values of the interaction energies in the (KS)I salt (calculated as $E = 1/2V(r)$[42]) for hydrogen-bonded and anion−π contacts (Table 1) are all in the 1.2 ± 0.2 kcal/mol range. This suggests a similar strength of anion−π and hydrogen bonds in (KS)I.

Overall, X-ray crystallography together with the QTAIM and NCI analyses showed that iodide anions form multiple anion−π and hydrogen bonds with the pyridinium cations in the solid state. However, the arrangements of cations and anions, and therefore intermolecular interactions, in this structure are also affected by crystal forces. Furthermore, the solid-state data alone do not indicate which interaction is responsible for the appearance of the charge-transfer absorption bands that were used by Kosower in his solvent polarity index "Z". To compare the modes of pairwise HyB and anion−π interactions taking place in solutions and to clarify the origin of the absorption bands, we carried out solution-phase studies of the complex formation between KS^+ cations and several anions, as well as computational analysis of their 1:1 complexes, as follows.

3.2. UV−Vis and NMR Studies of Complex Formation Between KS^+ and Anions in Liquid Phase. To explore the interactions of KS^+ with various anions in the liquid phase, we first prepared a salt of 1-ethyl-4-carbomethoxypyridinium cation with tetrakis (3,5-ditrifluoromethylphenyl)borate, commonly abbreviated as BArF (see Methods for details). The charge delocalization and shielding in these bulky non-coordinating anions minimize counterion interactions in their solid-state salt and solutions. The UV−vis spectrum of this snow-white salt is shown as a dashed red line in Figure 4. It contains a band with a maximum at 271 nm ($\varepsilon = 1.74 \times 10^4$ M^{-1} cm^{-1}), related to intramolecular transitions (vide infra), but does not show any absorption above 300 nm. This allows us to explore the appearance of absorption bands, if any,

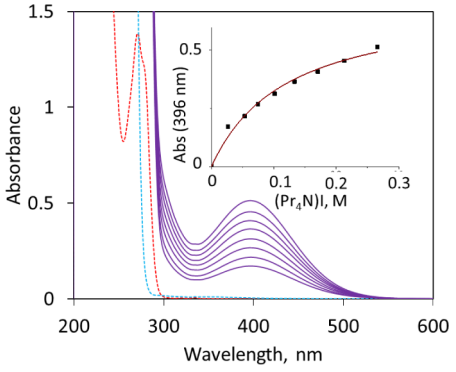

Figure 4. Spectra of the solutions containing various concentrations of $(Pr_4N)I$ and constant (4.0 mM) concentrations of (KS)BArF in acetonitrile (purple lines). Dashed red and blue lines show spectra of the individual solutions of (KS)BArF (0.8 mM) and $(Pr_4N)I$ (53 mM), respectively. Inset: dependence of the intensity of absorption at 396 nm on the concentration of iodide. The solid line shows a fit of the experimental data to the 1:1 binding isotherm.

https://doi.org/10.1021/acsomega.4c06750
ACS Omega 2024, 9, 43058−43067

occurring upon the addition of different anions to the solution of this salt.

The addition of iodide to a solution of the (KS)BArF resulted in the appearance of the absorption band in the 350−450 nm range. The wavelengths of the maximum of this band, λ_{max}, in various solvents (e.g., λ_{max} = 396 nm in acetonitrile) were consistent with those reported for (KS)I by Kosower.[16] In a solution with a constant concentration of KS^+ and variable concentrations of iodide, the intensity of this absorption band can be reasonably well fitted (inset in Figure 4) to the binding isotherm representing 1:1 complex formation between these reactants (eq 1):

$$KS^+ + I^- \rightleftarrows [KS^+,I^-] \quad (1)$$

However, due to the variation of ionic strength resulting from the increasing concentrations of $(Pr_4N)I$ in a series of these solutions, such fitting does not produce the thermodynamic equilibrium constant. The *apparent* value of $K = 8.5 \pm 1.4\ M^{-1}$ resulting from the fit in the inset of Figure 4 could be used only for a qualitative comparison of binding in similar systems.

Addition of Br^- or NCS^- anions to the solutions of (KS)BArF also resulted in the appearance of new absorption bands in the 300−400 nm range (Figure S3). Their maxima were blue-shifted as compared to that with iodide. Such a shift is consistent with the better electron-donor ability of the latter and the charge-transfer nature of the bands suggested by Kosower. In fact, energies of the absorption bands of the complexes formed by KS^+ followed the same Mulliken correlation with the difference of the redox potentials (which reflect the difference of their HOMOs and LUMOs energies in solutions) as for the earlier reported systems involving neutral π-acceptors (Figure 5).

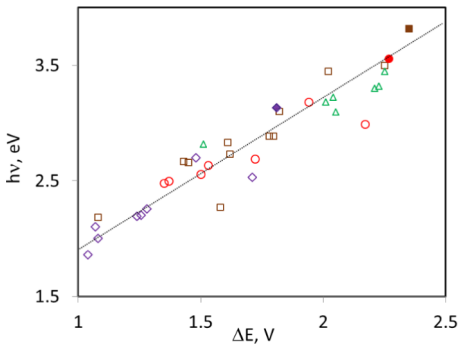

Figure 5. Mulliken correlation between energies of the absorption bands and the difference of the redox potentials of the reactants in the spectra of the complexes of iodide (purple rhombics), bromide (brown square), chloride (green triangles), and thiocyanate (red circles) with various π-acceptors. The filled symbols show data for the complexes with KS^+, while open symbols present previously published data with different π-acceptors (adapted from ref.[21]. Copyright 2019 American Chemical Society, see Table S4 for details).

The addition of chloride, which is a weaker electron donor, to the solution of (KS)BArf also increased absorption in the 300−350 nm range. However, due to the overlap of this new band with the absorption of KS^+ itself, only its tail was observed, which hindered the determination of its maximum. Finally, the spectra of the solution containing KS^+ and various concentrations of non-nucleophilic PF_6^- or ClO_4^- anions (which are very poor electron donors) were essentially the same as the spectrum of (KS)BArf (Figure S3). This dependence on the nature of anions was essentially the same as the results obtained earlier for the complexes with neutral tetracyanopyrazine or p-benzoquinone acceptors.[26]

Overall, the results of the UV−vis measurements of the interaction of KS^+ with different anions resembled the analogous data obtained with the π-acceptors in solutions where only anion−π complexes could be formed. It suggests a similar anion−π nature for these associations. Yet, the presence of hydrogen substituents in KS^+ and X-ray crystallographic data indicated that this cation can also form hydrogen-bonded complexes with iodide and other anions. In our previous study,[25] we utilized a combination of UV−vis and NMR measurements to differentiate and characterize hydrogen- and halogen-bonded complexes coexisting in solutions. As such, we turned to NMR measurements of the interaction of the anions with KS^+. Variations of the chemical shifts of the protons in the spectrum of (KS)BArF with concentration of added $(Pr_4N)I$ are illustrated in Figure 6.

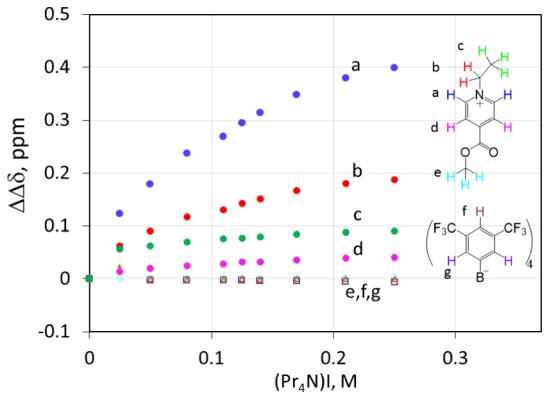

Figure 6. Variation of the chemical shifts of the ^1H signals in the NMR spectrum of (KS)I relative to the shift of each atom in pure (KS)I (10 mM, CD_3CN, 22 °C) with concentration of added iodide.

The data in Figure 6 indicated that the positions of the signals of the hydrogens from the methoxy group in KS^+ (and aromatic hydrogens in the BArF anions) were essentially independent of the concentration of the iodide. The positions of the hydrogen signals from the aromatic ring of KS^+ and its ethyl substituents were however all shifted downfield. Such a shift was related earlier to hydrogen bonding.[52] The largest magnitude of the shift was observed for the aromatic hydrogens in the ortho-position to the nitrogen, followed by those from the methylene group. This suggested that the iodine is hydrogen bonded mostly to these atoms, which is consistent with the arrangements of the anions in the (solid-state) X-ray structure. Thus, while UV−vis absorption data imply the formation of anion−π complexes, the NMR measurements suggested the presence of hydrogen bonding between anions and KS^+. To further elucidate the modes of interaction between KS^+ and iodide, as well as solvent dependence of the characteristics of these complexes, we carried out a computational analysis of these associations.

3.3. Computational Analysis of Complexes Between Iodide and KS^+. Recent developments of the σ-hole and π-hole concepts demonstrated that the surface electrostatic potentials represent a useful tool in the analysis of the various supramolecular interactions.[53] As illustrated in Figure 1, the maximum values of this potential on the surface of KS^+ are

https://doi.org/10.1021/acsomega.4c06750
ACS Omega 2024, 9, 43058−43067

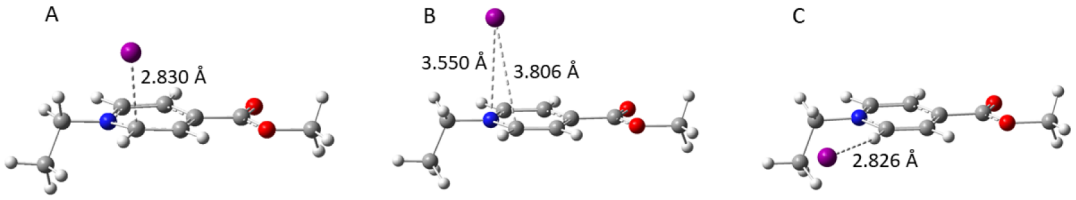

Figure 7. Calculated structures of the anion−π (A, B) and hydrogen-bonded (C) complexes between KS^+ and I^- optimized in the gas-phase (A) and acetonitrile (B, C).

Table 2. Characteristics of the Anion−π and HyB Complexes of KS^+ with Various Anions in Acetonitrile

	HyB complex (Calc)			Anion−π complex (Calc)			
Anion	ΔE, kcal/mol	λ_{max}, nm	Δq,[a] e	ΔE, kcal/mol	λ_{max}, nm	Δq,[a] e	λ_{max}, nm (Exp)
I^-	−5.3	338	0.026	−5.1	390	0.008	396
Br^-	−6.5	302	0.032	−5.1	346	0.009	324
NCS^-	−5.8	321	0.021	−10.2	355	0.010	354

[a]Anion-to-KS^+ charge-transfer (from NBO calculations[55]).

located between the methylene and aromatic hydrogens (in ortho-position relative to the nitrogen atom) on the face of the aromatic ring with a potential about 10% lower than that observed on its side. Optimization in the gas phase, however, produced dyads in which anions were located over the face of the aromatic ring regardless of the starting geometries of the associations (which were extracted from the X-ray structures) in which iodides were positioned either over the face or on the side of the aromatic ring (such results is probably related to the contributions of different intermolecular forces in anion−π bonding.[54] The optimization with acetonitrile as a medium produced local minima corresponding to the anion−π (with anion over the face of the ring) and hydrogen-bonded complexes (Figure 7).

The structures of the anion−π and HyB complexes of pyridinium and iodide optimized in acetonitrile were generally consistent with the mutual arrangements of the species in the solid-state X-ray structure. The energies of these two complexes were very close (Table 2).

This similarity in energies of the anion−π and hydrogen-bonded complexes is also consistent with the observation of both types of interactions in the solid state. It also implies the coexistence of both anion−π and HyB complexes in solutions. This suggestion is supported by the comparison of the experimental results of the UV−vis and NMR measurements with the calculated NMR shifts and UV−vis spectra.

The calculated values of the chemical shifts in the HyB and anion−π complexes relative to the values in the individual KS^+ are listed in Table 3 (note that these numbers represent averaged values over all equivalent protons, see individual shifts in Table S5).

The calculations showed that the chemical shifts of the protons involved in hydrogen bonding with iodide (Figure 7C) are shifted to higher ppm values than in the individual KS^+. The signals of the hydrogens that are not involved in HyB in such complexes are shifted to the slightly lower values. Similar small shifts to the lower ppm values are found for the hydrogens in the anion−π complex. In the experimental spectrum, however, all signals are either shifted to larger ppm values or remained essentially unchanged. These differences are apparently related to the presence in solutions of the several anion−π and HyB complexes with the distinct structures and the fact that the HyB-induced polarization

Table 3. Calculated and Experimental Chemical Shifts (in ppm, Relative to the Signal in the Individual KS^+)

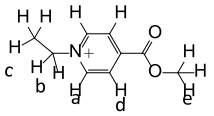

Hydrogen[a]	a	b	c	d	e
anion−π complex(Calc)	−0.09	−0.01	−0.02	−0.08	−0.02
HyB complex(Calc)	2.88	1.08	0.06	−0.16	−0.02
experimental[b]	0.40	0.19	0.09	0.04	0.00

[a]See the structure above. [b]Solution of 10 mM of KS^+ and 0.25 M iodide in CD_3CN.

leads to the larger downfield shifts of the bonded protons and smaller upfield shift of the neighboring protons. As such, the larger downfield (positive) shifts of protons a and b indicates that the calculated (most stable) structure in Figure 7C (which is characterized by such shifts) is indeed a prevailing HyB complex in solutions. However, there are likely also a fraction of the HyB complexes in which iodide is bonded to hydrogen d. This HyB complex is characterized by a larger downfield (positive) shift of a proton d, and smaller upfield shift of proton a (see Table S5). The presence of such HyB complex decreases experimentally measured shift of the proton a and results in the small positive downfield shift of the proton d. Furthermore, since the anion−π complexes in solution are characterized by minimal negative shifts of the signals and the experimental shifts of protons a and b are much lower than the calculated ones, these data is not sufficient to confirm or to exclude the presence of anion−π complexes in the solutions. To see if their presence can be supported by the UV−vis data, we turned to a comparison of experimental results with TD DFT calculations.

The data in Table 2 indicate that the absorption bands measured experimentally in the solutions of KS^+ and iodide$^-$ or NCS^- are very close to those calculated for the anion−π complexes with these anions. The calculated absorption band maxima for the HyB complexes with these anions are shifted substantially to lower wavelengths. On the other hand, the experimental value of λ_{max} for the complex with bromide is approximately in the middle between the values calculated for the corresponding anion−π and HyB complexes. To further

https://doi.org/10.1021/acsomega.4c06750
ACS Omega 2024, 9, 43058−43067

clarify the assignment of the absorption bands, we calculated absorption band maxima for the HyB and anion−π complexes of (KS)I in various solvents and compared them with the experimental values reported by Kosower. The interaction energies and UV−vis spectral data for (KS)I are listed in Tables S6 and S7. They show that the average difference between experimental and calculated values for the anion−π complexes of 0.11 eV is more than three times smaller than for the hydrogen-bonded complexes (0.36 eV). The close inspection of the results of the TD calculations also showed that the most significant difference between the experimental values or λ_{max} and the values calculated for the anion−π complexes were observed in protic (i.e., the hydrogen-bond donating) solvents, such as alcohols. Furthermore, the calculated energies of the charge-transfer transitions in these solvents were substantially lower than the experimental values. To check if the energies of these transitions are affected by the hydrogen bonding of anions with solvent molecules (which is not taken into account by the PCM solvation model), we carried out calculations of the systems in which three methanol molecules were added to the $KS^+ \cdot I^-$ pairs. Such calculations produced minima in which anions were additionally hydrogen bonded with three methanol molecules (Figure S5). The absorption band energies resulting from the TD DFT calculations of such complexes were substantially higher than those calculated without solvent molecules. Most importantly, the calculated absorption band energies of the anion−π complex in which anions were also involved in hydrogen bonding with solvent were close to the experimental values. On the other hand, TD DFT calculations of the corresponding association in which anion was hydrogen bonded with pyridinium and solvent molecules produced absorption band with much higher energies which overlapped with the absorption band of the pyridinium. All these data corroborate the suggestion (vide supra) that the absorption band with λ_{max} = 396 nm in the UV−vis spectra of the solutions of KS^+ and iodide in acetonitrile is related to the anion−π complexes. The shape of this band is well fit to a single Gaussian function above λ > 370 nm. As such, while HyB complex can contribute somewhat to the absorption in the 300−350 nm range, the variation of the intensity at 396 nm (vide supra) is related solely to the changes in concentration of the anion−π complex.

Finally, to compare the solvent dependences of the charge-assisted HyB and anion−π complexes between KS^+ and iodide with those involving neutral TCB molecules, we calculated the binding energies, ΔE, of all these complexes in various solvents. The variations of the ΔE values with the dielectric constant of the medium are illustrated in Figure 8 (see details in Tables S2 and S6).

These calculations reveal several tendencies. First, the dependencies of the calculated binding energies of the anion−π and HyB complexes between iodide and pyridinium on the value of the dielectric constant of the medium are much steeper than those of the corresponding associations involving neutral π-acceptors. As such, while the magnitude of ΔE for KS^+ I^- in low polar media are much higher than that of the complexes with TCB, the energy of all complexes in polar solvents are close to each other. As was described in our earlier study, the variations of the interaction energies of the anion−π complexes with the neutral π-acceptors are well accounted for by the Born model (in which the difference of the solvation energies of the individual and bonded anions are related to the

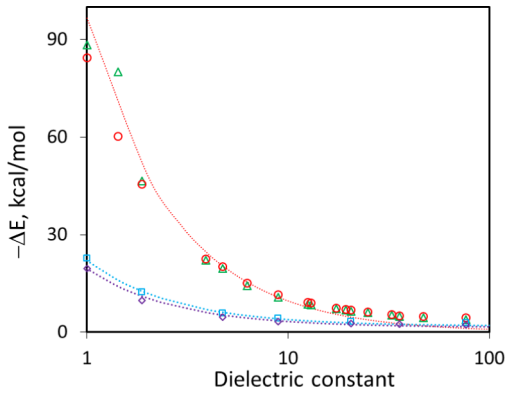

Figure 8. Dependencies of the binding energies between I^- and KS^+ or TCB in their anion−π and HyB complexes on the dielectric constant of the medium. Red circles and green triangles show values for HyB and anion−π complexes between I^- and KS^+, respectively, and the dotted red line shows interaction energy between two unity charges separated by 3.6 Å. Purple rhombics and blue squares show values for the HyB and anion−π complexes, respectively, between I^- and TCB (blue and purple dotted lines show fitting of these energies using the Born solvation model).

higher effective solvation radii of the latter.[56] According to the Born model, the free energy of solvation is approximated as

$$\Delta G = -N_A z^2 e^2/(8\varepsilon_0 r) \times (1 - 1/\varepsilon_r) \quad (2)$$

where N_A is the Avogadro number, z and e are the charge of an ion and the elementary charge, ε_0 is the permittivity of vacuum, r is the effective radius of the ion and ε_r is the dielectric constant of the solvent.[57] Assuming that the changes in ΔE are determined by the variations in the solvation energies of the anion−π complex and the free halide anion (both with z = 1), and that the effective radii of the individual anion (r_X) and anion in the complex (r_π) remain approximately constant, the ΔE values in the different solvents can be expressed as

$$\Delta E = \Delta E^v - N_A e^2/(8\varepsilon_0) \times (1 - 1/\varepsilon_r)(1/r_\pi - 1/r_X) \quad (3)$$

where ΔE^v represents the value calculated in vacuum. The dotted blue and violet lines in Figure 8 show variations of ΔE with ε_r for both HaB and the anion−π complexes obtained by fitting of the calculated values with the effective radii of iodide r_X and that of complex r_π as adjustable parameters. The good fit obtained with r_X of 2.10 Å and r_π of 2.40 Å for the anion−π and 2.36 Å for the HyB complex confirms that variations of the strength of the anion−π complexes in various media are well accounted by the Born model

In contrast to the complexes with the neutral π-acceptor, the changes in the energies of the charge-assisted KS^+ I^- complexes follow (roughly) those between two unity charges separated by about 3.6 Å (red dotted line in Figure 8). However, the deviations from this line to the larger magnitudes of the interaction energies in polar solvents suggest that binding in these complexes involves additional components that do not decrease as fast with the increase in dielectric constant. The presence of such a specific interaction is supported by the fact that while the anion−π complexes are somewhat more stable in media with very low polarity than the HyB associations, the latter become slightly more stable in the moderately polar and very polar solvents. It should be noted, however, that many polar solvents are also good HyB donors, and the energetics of the interaction of anions with pyridinium

https://doi.org/10.1021/acsomega.4c06750
ACS Omega 2024, 9, 43058−43067

can be substantially affected by hydrogen bonding between the anions and the solvent molecules. For example, the HyB complexes between KS^+ and I^- calculated using the PCM model in methanol are more stable than the corresponding anion−π complexes by about 0.2 kcal/mol. However, if anions are also hydrogen-bonded with three methanol molecules, the anion−π complex between iodide and KS^+ is more stable than the HyB association by 3.5 kcal/mol (see Figure S5). This confirms that the use of an implicit solvation model for the comparison of different modes of supramolecular interactions involving anions might be misleading.

4. CONCLUSIONS

Combined experimental and computational studies showed a coexistence and a comparable strength of anion−π and hydrogen bonding between iodide and the 1-ethyl-4-carbomethoxypyridium cation in the solid state and in solution. The studies also indicated that the shifts of the signals in the ^{1}H NMR spectra of KS^+ are determined primarily by its hydrogen bonding with anions, but the (charge-transfer) absorption bands in the UV−vis spectra (which were used by Kosower as a solvent polarity probe) are related to the anion−π interaction between iodide and this cationic π-acceptor. Importantly, while the variations of the interaction energies of anions with the neutral π-acceptors are described well by the Born solvation model, the strength of the bonding in the charge-assisted complexes is mostly determined by the electrostatic attraction of the cationic and anionic reactants (This conclusion is consistent with the small values of charge-transfer in the complexes obtained via NBO calculations[58] related to interaction of lone pairs of anions with antibonding orbitals of KS^+, see Table 2). Still, a subtle variation in the strength of these interactions results in an interchange of the relative stabilities of the HyB and anion−π complexes with an increase of dielectric constant. The calculations also showed a switch of the relative stabilities of the HyB and anion−π complexes when solvent molecules were explicitly added to the systems evaluated using a polarizable continuum model, underlining limitations of PCM for the estimation of the energetics of the supramolecular bonding, at least in protic solvents.

■ ASSOCIATED CONTENT

Supporting Information

The Supporting Information is available free of charge at https://pubs.acs.org/doi/10.1021/acsomega.4c06750.

Experimental crystallographic and spectral data, as well as details of calculations (PDF)

CCDC 2344693 (CIF)

CCDC 2344694 (CIF)

■ AUTHOR INFORMATION

Corresponding Author

Sergiy V. Rosokha − *Department of Chemistry, Ball State University, Muncie, Indiana 47306, United States;* orcid.org/0000-0003-3172-8523; Email: svrosokha@bsu.edu

Authors

Emmanuel Bitega − *Department of Chemistry, Ball State University, Muncie, Indiana 47306, United States*

Reva Patil − *Department of Chemistry, Ball State University, Muncie, Indiana 47306, United States*

Matthias Zeller − *Department of Chemistry, Purdue University, West Lafayette, Indiana 47907, United States;* orcid.org/0000-0002-3305-852X

Complete contact information is available at: https://pubs.acs.org/10.1021/acsomega.4c06750

Notes

The authors declare no competing financial interest.

■ ACKNOWLEDGMENTS

We thank the National Science Foundation (grant CHE-2003603) for the financial support of this work. Calculations were done on Ball State University's beowulf cluster, which is supported by the National Science Foundation (MRI-1726017) and Ball State University. X-ray measurements were supported by the National Science Foundation through the Major Research Instrumentation Program under Grant No. CHE 1625543 (funding for the single crystal X-ray diffractometer).

■ REFERENCES

(1) Frontera, A.; Gamez, P.; Mascal, M.; Mooibroek, T. J.; Reedijk, J. Putting anion-π interactions into perspective. *Angew. Chem., Int. Ed.* **2011**, *50*, 9564−9583.

(2) Quinonero, D.; Garau, C.; Rotger, C.; Frontera, A.; Ballester, P.; Costa, A.; Deya, P. M. Anion-πinteractions: Do they exist? *Angew. Chem., Int. Ed.* **2002**, *41*, 3389−3392.

(3) Mascal, M.; Armstrong, A.; Bartberger, M. D. Anion-aromatic bonding: a case for anion recognition by π-acidic rings. *J. Am. Chem. Soc.* **2002**, *124*, 6274−6276.

(4) Alkorta, I.; Rozas, I.; Elguero, J. Interaction of anions with perfluoro aromatic compounds. *J. Am. Chem. Soc.* **2002**, *124*, 8593−8598.

(5) Schottel, B. L.; Chifotides, H. T.; Dunbar, K. R. Anion-π Interactions. *Chem. Soc. Rev.* **2008**, *37*, 68−83.

(6) Giese, M.; Albrecht, M.; Rissanen, K. Experimental investigation of anion-π interactions - applications and biochemical relevance. *Chem. Commun.* **2016**, *52*, 1778−1795.

(7) Wang, D.-X.; Wang, M.-X. Exploring anion−π interactions and their applications in supramolecular chemistry. *Acc. Chem. Res.* **2020**, *53*, 1364−1380.

(8) Rosokha, S. V. Anion-π Interactions: What's in the Name? *ChemPluschem* **2023**, *88* (8), No. e202300350.

(9) Briegleb, G.; Liptay, W.; Fick, R. Electron exchange; interaction of anions with organic electron acceptors. II. Halide ions with s-trinitrobenzene. *Z. Elektrochem* **1962**, *66*, 851−858.

(10) Briegleb, G.; Liptay, W.; Fick, R. Electron exchange; interaction of anions with organic electron acceptors. III. Bromide-, iodide-, and thiocyanate-ions with tetracyanoethylene, chloranil, bromanil, iodanil. *Z. Elektrochem* **1962**, *66*, 859−862.

(11) Davis, K. M. C. Charge-transfer complexes. Solvent shifts of the charge-transfer band of complexes formed between halide ions and organic electron acceptors. *J. Chem. Soc. B* **1967**, 1128−1130.

(12) Benesi, H. A.; Hildebrand, J. H. A spectrophotometric investigation of the interaction of iodine with aromatic hydrocarbons *J. Am. Chem. Soc.* **1949**, *71*, 2703−2707.

(13) Hassel, O. Structures of electron-transfer and related molecular complexes in the solid state. *Mol. Phys.* **1958**, *1*, 241−246.

(14) Mulliken, R. S.; Person, W. B. *Molecular Complexes: A Lecture and Reprint*; Wiley: New York, 1969.

(15) Foster, R. *Organic Charge-Transfer Complexes*; Academic: New York, 1969.

(16) Kosower, E. M. The effect of solvent on spectra. I. A new empirical measure of solvent polarity-Z-values. *J. Am. Chem. Soc.* **1958**, *80*, 3253−3260.
(17) (a) Koplitz, L. V.; Bay, K. D.; DiGiovanni, N.; Mague, J. T. The influence of weak hydrogen bonds on the properties of 3-cyano-n-methylpyridinium chloride and iodide. *J. Chem. Crystallogr.* **2003**, *33*, 391−402. (b) García, M. D.; Blanco, V.; Platas-Iglesias, C.; Peinador, C.; Quintela, J. M. Interplay between halogen/hydrogen bonding and electrostatic interactions in 1,1′-bis(4-iodobenzyl)-4,4′-bipyridine-1,1′-diium salts. *Cryst. Growth Des.* **2009**, *9*, 5009−5013. (c) Deschner, J.; Choczynski, J. M.; Wong, C. Y.; Hayes, K. L.; Crisci, R. R.; Lasher, E.; Dragonette, J.; Cardenas, A. J. P. 1,4-Dimethylpyridinium iodide. *IUCrData* **2017**, *2*, x170269. (d) Fotovič, L.; Stilinovič, V. Halogen bonding in n-alkyl-3-halogenopyridinium salts. *Crystals* **2021**, *11*, 1240.
(18) Berryman, O. B.; Bryantsev, V. S.; Stay, D. P.; Johnson, D. W.; Hay, B. P. Structural criteria for the design of anion receptors: the interaction of halides with electron-deficient arenes. *J. Am. Chem. Soc.* **2007**, *129*, 48−58.
(19) Wilson, J.; Maxson, T.; Wright, I.; Zeller, M.; Rosokha, S. Diversity and uniformity in anion-π complexes of thiocyanate with aromatic, olefinic and quinoidal π-acceptors. *Dalton Trans.* **2020**, *49*, 8734−8743.
(20) Mohammad, M.; Khan, A. Y.; Iqbal, M.; Iqbal, R.; Razzaq, M. Pyridinyl radical, pyridinyl anions, Z values, and disproportionation equilibria. *J. Am. Chem. Soc.* **1978**, *100*, 7658−7660.
(21) Kepler, S.; Zeller, M.; Rosokha, S. V. Anion−π Complexes of Halides with p -Benzoquinones: Structures, Thermodynamics, and Criteria of Charge Transfer to Electron Transfer Transition. *Am. Chem. Soc.* **2019**, *141*, 9338−9348.
(22) *Bruker Apex3 v2016.9−0, SAINT V8.37A*; Bruker AXS Inc.: Madison, WI, 2016.
(23) (a) Sheldrick, G. *SHELXTL suite of programs, Version 6.14, 2000−2003*; Bruker AXS Inc.: Madison, WI, 2003. (b) Sheldrick, G. Crystal Structure Refinement with SHELXL. *Acta Cryst. C* **2015**, *71*, 3−8.
(24) Hübschle, C.; Sheldrick, G.; Dittrich, B. ShelXle: a Qt Graphical User Interface for SHELXL. *J. Appl. Crystallogr.* **2011**, *44*, 1281−1284.
(25) Watson, B.; Grounds, O.; Borley, W.; Rosokha, S. V. Resolving halogen vs hydrogen bonding dichotomy in solutions: Intermolecular complexes of trihalomethanes with halide and pseudohalide anions. *Phys. Chem. Chem. Phys.* **2018**, *20*, 21999−22007.
(26) Odubo, F. E.; Zeller, M.; Rosokha, S. V. Exploring the Nature of Anion-π Interactions: Complexes of p-Acceptors with Fluoro- or Oxoanions Compared to the Associations with Halides. *J. Phys. Chem. A* **2023**, *127* (28), 5851−5859.
(27) Strauss, S. H. The search for larger and more weakly coordinating anions. *Chem. Rev.* **1993**, *93*, 927−942.
(28) Krossing, I.; Reisinger, A. Chemistry with weakly-coordinating fluorinated alkoxyaluminate anions: Gas phase cations in condensed phases? *Coord. Chem. Rev.* **2006**, *250*, 2721−2744.
(29) Frisch, M. J.; Trucks, G. W.; Schlegel, H. B.; Scuseria, G. E.; Robb, M. A.; Cheeseman, J. R.; Scalmani, G.; Barone, V.; Mennucci, B.; Petersson, G. A., et al. *Gaussian 09, Revision C.01*; Gaussian, Inc.: Wallingford CT, 2009.
(30) Zhao, Y.; Truhlar, D. G. The M06 suite of density functionals for main group thermochemistry, thermochemical kinetics, noncovalent interactions, excited states, and transition elements: two new functionals and systematic testing of four M06-class functionals and 12 other functionals. *Theor. Chem. Acc.* **2008**, *120*, 215−241.
(31) Weigend, F.; Ahlrichs, R. Balanced basis sets of split valence, triple zeta valence and quadruple zeta valence quality for H to Rn: Design an assessment of accuracy. *Phys. Chem. Chem. Phys.* **2005**, *7*, 3297−3305.
(32) Tomasi, J.; Mennucci, B.; Cammi, R. Quantum mechanical continuum solvation models. *Chem. Rev.* **2005**, *105*, 2999.
(33) Zhu, Z.; Xu, Z.; Zhu, W. Interaction nature and computational methods for halogen bonding: a perspective. *J. Chem. Inf. Model.* **2020**, *60*, 2683.
(34) Wang, K.; Lv, J.; Miao, J. Assessment of density functionals and force field methods on anion−π interaction in heterocyclic calix complexes. *Theor. Chem. Acc.* **2015**, *134*, 5.
(35) Bauzá, A.; Quiñonero, D.; Deyà, P. M.; Frontera, A. Is the use of diffuse functions essential for the properly description of noncovalent interactions involving anions? *J. Phys. Chem. A* **2013**, *117*, 2651−2655.
(36) Bader, R. F. W. A quantum theory of molecular structure and its applications. *Chem. Rev.* **1991**, *91*, 893−928.
(37) Popelier, P. L. A. *The QTAIM perspective of chemical bonding in The Chemical Bond*; John Wiley & Sons, Ltd, 2014; p 271.
(38) Johnson, E. R.; Keinan, S.; Mori-Sánchez, P.; Contreras-García, J.; Cohen, A. J.; Yang, W. Revealing noncovalent interactions. *J. Am. Chem. Soc.* **2010**, *132*, 6498−6506.
(39) Lu, T.; Chen, F. Multiwfn: a multifunctional wavefunction analyzer. *J. Comput. Chem.* **2012**, *33*, 580−592.
(40) Humphrey, W.; Dalke, A.; Schulten, K. V. Visual Molecular Dynamics. *J. Mol. Graphics* **1996**, *14*, 33.
(41) Bondi, A. van der Waals volumes and radii. *J. Phys. Chem.* **1964**, *68*, 441−451.
(42) Espinosa, E.; Molins, E.; Lecomte, C. Hydrogen bond strengths revealed by topological analyses of experimentally observed electron densities. *Chem. Phys. Lett.* **1998**, *285*, 170−173.
(43) Hay, B. P.; Custelcean, R. Anion−π interactions in crystal structures: commonplace or extraordinary? *Cryst. Growth Des.* **2009**, *9*, 2539−2545.
(44) Espinosa, E.; Alkorta, I.; Elguero, J.; Molins, E. From weak to strong interactions: a comprehensive analysis of the topological and energetic properties of the electron density distribution involving X−H···F−Y systems. *J. Chem. Phys.* **2002**, *117*, 5529.
(45) Cremer, D.; Kraka, E. A Description of the chemical bond in terms of local properties of electron density and energy. *Croat. Chem. Acta* **1984**, *57*, 1259−1281.
(46) (a) Miller, D. K.; Chernyshov, I. Y.; Torubaev, Y. V.; Rosokha, S. V. From weak to strong interactions: structural and electron topology analysis of the continuum from the supramolecular chalcogen bonding to covalent bonds. *Phys. Chem. Chem. Phys.* **2022**, *24*, 8251−8259. (b) Miller, D. K.; Loy, C.; Rosokha, S. V. Examining a transition from supramolecular halogen bonding to covalent bonds: topological analysis of electron densities and energies in the complexes of bromosubstituted electrophiles. *ACS Omega* **2021**, *6*, 23588−23597.
(47) Chernyshov, I. Y.; Ananyev, I. V.; Pidko, E. A. Revisiting van der Waals radii: from comprehensive structural analysis to knowledge-based classification of interatomic contacts. *ChemPhyschem* **2020**, *21*, 370−376.
(48) Grabowski, S. J. Hydrogen bonding strength—measures based on geometric and topological parameters. *J. Phys. Org. Chem.* **2004**, *17*, 18−31.
(49) Vener, M. V.; Egorova, A. N.; Churakov, A. V.; Tsirelson, V. G. Intermolecular hydrogen bond energies in crystals evaluated using electron density properties: DFT computations with periodic boundary conditions. *J. Comput. Chem.* **2012**, *33*, 2303−2309.
(50) Kuznetsov, M. L. Relationships between Interaction Energy and Electron Density Properties for Homo Halogen Bonds of the $[(A)_nY-X\cdots X-Z(B)_m]$ Type (X = Cl, Br, I). *Molecules* **2019**, *24*, 2733.
(51) Scheiner, S. Transition between the Noncovalency and Covalency of σ−Hole Bonds. *J. Phys. Chem. A* **2023**, *127*, 9760−9770.
(52) Green, R. D.; Martin, J. S. Anion-molecule complexes in solution. I. Nuclear magnetic resonance and infrared studies of halide ion-trihalomethane association *J. Am. Chem. Soc.* **1968**, *90*, 3659−3668.
(53) Bauzá, A.; Mooibroek, T. J.; Frontera, A. The Bright Future of Unconventional σ/π-Hole Interactions. *ChemPhyschem* **2015**, *16*, 2496−2517.

https://doi.org/10.1021/acsomega.4c06750
ACS Omega 2024, 9, 43058−43067

(54) Liu, Z.; Chen, Z.; Xi, J.; Xu, X. An accurate single descriptor for ion−π interactions. *Natl. Sci. Rev.* **2020**, *7* (6), 1036−1045.
(55) Weinhold, F.; Landis, C. R. *Discovering Chemistry with Natural Bond Orbitals*; Wiley: Hoboken, NJ, 2012.
(56) Howe, D.; Wilson, J.; Rosokha, S. V. Solvent and ionic atmosphere effects in anion-π interactions: complexes of halide anions with p-benzoquinones. *J. Phys. Chem. A* **2022**, *126*, 4255−4263.
(57) (a) Born, M. Volumen und hydratationswärme der ionen. *Z. Physik* **1920**, *1*, 45−48. (b) Atkins, P.; De Paula, J.; Keeler, J. *Physical Chemistry*, 11 th ed.; Oxford University Press, 2018.
(58) (a) Grabowski, S. J. What is the covalency of hydrogen bonding? *Chem. Rev.* **2011**, *111*, 2597−2625. (b) Khaliullin, R. Z.; Cobar, E. A.; Lochan, R. C.; Bell, A. T.; Head-Gordon, M. Unravelling the origin of intermolecular interactions using absolutely localized molecular orbitals. *J. Phys. Chem. A* **2007**, *111*, 8753−8765.

https://doi.org/10.1021/acsomega.4c06750
ACS Omega 2024, 9, 43058−43067